

CREATING COMPLEX HOLLOW METAL GEOMETRIES USING ADDITIVE MANUFACTURING AND ELECTROFORMING

D. L. McCarthy and C. B. Williams

DREAMS Lab, Department of Mechanical Engineering
Virginia Tech, Blacksburg, VA 24061

REVIEWED, Accepted August 22, 2012

ABSTRACT

Additive manufacturing introduces a new design paradigm that allows the fabrication of geometrically complex parts that cannot be produced by traditional manufacturing and assembly methods. In this paper, the authors investigate the combination of laser sintering with an electroforming process using electroless nickel plating to produce complex, thin-walled, hollow, metal geometries. The resulting geometries cannot be produced directly with other additive manufacturing systems. The resulting process is used to produce a cellular nickel structure featuring 800 μ m walls that is 65 vol% air from a polyamide substrate with 3mm pores.

Keywords: Additive Manufacturing, Electroless Plating, Electroforming, Laser Sintering

1. INTRODUCTION

1.1. Motivation

Past work has shown that the use of hollow members in applications like high strength-to-weight ratio sandwich panel structures can have significant benefits, including improvements to the peak compressive collapse strength and inelastic buckling resistance [1]. In general, sandwiched trussed structures are typically made with a folding and brazing operation on a diamond perforated metal sheet. In structures featuring hollow tubes, the same approach is taken, but instead by bending an arrayed series of hollow metal tubes. In both cases, the resulting structures are limited to planar macrostructures, and a limited set of mesostructure geometries that can be shaped via bending.

To address these geometric constraints, the authors look to additive manufacturing (AM) as a means of providing the freedom necessary for a designer to create complex hollow metal cellular artifacts with a designed mesostructure. Combining the benefits of hollow structures with the design complexity provided by additive manufacturing increases the range of potential applications, including more advanced high strength-to-weight ratio structures. In addition, as hollow members enable the transmission of fluids, the resultant high-surface area structures could be used as heat exchangers.

1.2. Metal Additive Manufacturing

As the mechanical properties and heat conductivity of metals make them ideal for these applications, metal AM processes are candidates for providing the desired complex hollow geometries. Direct metal AM processes (e.g., direct metal laser sintering, selective laser melting, and electron beam melting) tend to provide a rough surface, which may cause problems for applications involving fluid flow. Additionally, the majority of the metals that can be used in these processes have poor heat conductivity [2, 3], excepting aluminum (which provides its own

difficulties due to poor flowability and high reflectivity [4]). High heat conductivity metals like copper could theoretically be used, but that conductivity actually acts against the system, lowering part accuracy and increasing part growth due to the uncontrollable melt pool and solidification process [5]. Both copper and aluminum also experience major oxidation issues during sintering, which restricts diffusion and reduces the wettability of the surface [4].

Indirect metal processes (e.g., two-phase selective laser sintering and three-dimensional printing) require involved post-processing that can be difficult for complex structures. Small-scale truss structures, for instance, are not producible with indirect metal 3D printing because of the weakness of the green part after printing before post-processing. Attempting to produce a truss structure with hollow members is impossible primarily due to powder removal requirements while the part is still weak. Additionally, infiltrating complex thin walls with another metal during post-processing is difficult.

Both direct and indirect powder bed fusion processes like those described require powder removal which is difficult or impossible for long, hollow channels in complex structures. Additionally, the available resolutions of these processes do not allow the creation of thin walls (on the order of 100 μ m) with reliable structural integrity.

1.3. Hybrid Manufacturing Approach

While current metal AM systems might be able to produce complex hollow metal geometries, the resultant geometries are limited by the laser spot size. For example, the wall thickness of hollow geometries cannot be smaller than the laser spot diameter. To provide more flexibility in the design and realization of complex hollow geometries, the authors propose a hybrid electroforming approach wherein additively manufactured thermoplastics are used as sacrificial substrates that are removed once they have been plated in metal, leaving behind the thin walls of the metal plate. A generalized representation of the proposed hybrid process is shown in Figure 1.

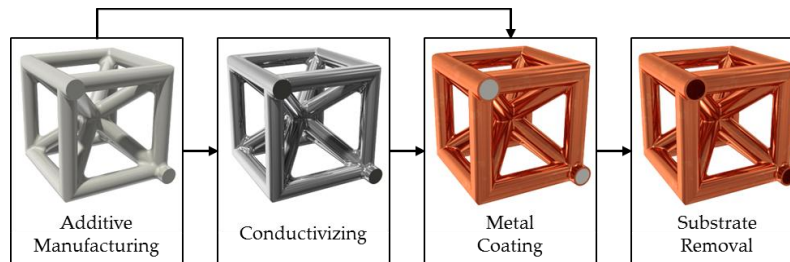


Figure 1. Diagram of the generalized proposed process by sub-function for producing complex, hollow, metal geometries.

Several groups have used similar approaches in the past (though most only in part). Chandrasekhar [6], Saleh [7], Zhou [8], and their respective coauthors all used an approach that used stereolithography (SL) or laser sintering (LS), electroless plating, and electroplating to produce plated parts from AM substrates. Their goals were to improve the mechanical properties of the AM parts by adding a layer of metal coat. These studies addressed only simple geometries (i.e., airfoils and tensile testing “dog bones”) without the complex internal features desired for this work. Additionally, they do not consider substrate removal procedures.

Markkula and coauthors [9] investigated the use of fused deposition modeling (FDM), electroless plating, and electroplating to produce high strength-to-weight ratio sandwich trusses. They tested pyramidal, tetrahedral, and strut-reinforced tetrahedral (SRT) truss formations and compared their compressive properties. Despite being truss structures, the process was simplified by producing only a single truss cell for each test, which does not require consideration of geometric dependencies in the plating process. This procedure also did not include any substrate removal process.

Monzón and coauthors [10] used FDM, electroless plating, electroplating, and mechanical separation to produce electrically conductive patterns for various applications. They have also explored using FDM in an electroforming context to make low quality injection molds for rapid tooling [11]. Their research focused on taking advantage of the internal stresses in FDM parts to reduce the adhesion between the electroless coat and AM substrate. The parts were simple, allowing for mechanical separation of the AM substrate from the metal coat while preserving both the substrate and the electroform.

The rapid tooling of electric discharge machining (EDM) electrodes accounts for the majority of research involving the use of AM substrates in a complete electroforming process. Most researchers select SL as the AM process of choice because of its high resolution and smooth surface finish. Arthur and coauthors [12] used conductive paint, electroplating, and tested both thermal (burnout) and chemical (etching) substrate removal. Yang and Leu [13, 14] used electroless plating, electroplating, and thermal substrate removal. These groups concluded that thermal substrate removal has significant negative effects on the quality of the electroform due to the volatility of the SL photopolymers. Work by Gillot [15], Dimla [16], and their respective coauthors concluded that electroplating is too geometrically dependent to be used in this process, showing considerable non-uniformity, affecting the conductivity of the electrode.

The design of a new AM-inspired process for creating microlattice structures from SL photopolymers [17, 18] led to a process that combined an SL-like process with electroless plating and chemical etching from Schaedler and coauthors [19] to produce ultralight metallic microlattices. The resultant geometries were limited to straight-lined truss structures with limited dimensions, not taking advantage of the design freedom provided by AM. Additionally, since the properties of these structures are specific to the nanocrystalline electrodeposition of the nickel used [20], producing copper structures to improve heat and electrical conductivity requires a different process that would likely not be able to replicate the structural recovery properties of the nanocrystalline nickel.

1.4. Design Goals

While past hybrid AM/metal plating processes have successfully produced high quality metal coatings on printed polymers, considerable effort remains to finalize the proposed hybrid process chain (Figure 1). A successful hybrid process will be able to produce complex, hollow, metal geometries with the full design freedom provided by AM. The manufactured structures must be exclusively metal (preferably with high heat conductivity), be self-supporting, and be producible with any level of design complexity. Ideally, the developed process would be relatively inexpensive and be possible in a lab setting, without requiring outsourcing or extensive knowledge of complicated processes.

Section 2 discusses process selection, using a morphological chart to investigate process combinations and eliminate unhelpful solutions for each process sub-function. Section 3 details the procedure used to produce a complex, hollow, metal geometry. Section 4 provides the results and analysis of a part after completing the process. Section 5 concludes the work with the contributions and limitations as well as the recommendations for future work.

2. PROCESS SELECTION

Figure 2 shows a morphological chart based on the sub-functions presented in the generalized process diagram in Figure 1. It is populated with potential solutions for each sub-function. Identifying combinations with one solution from each sub-function helps to provide process alternatives that might otherwise be missed. In this section, these potential solutions are investigated and most are eliminated to narrow the experimental scope.

		Solutions				
Sub-Functions	Additive Manufacturing	Selective Laser Sintering (SLS)	Fused Deposition Modeling (FDM)	Direct Inkjet 3D Printing (3DP)	Stereolithography (SL)	
	Conductivizing	AgNO ₃ to Ag ₂ S Conversion	Conductive Paint (Silvaspray™)	Electroless Plating	None	
	Metal Coating	Electroplating	Vacuum Metallization	Metal Spraying	Cathode Sputtering	Electroless Plating
	Substrate Removal	Burnout (Thermal)		Etching (Chemical)		Separation (Mechanical)

Figure 2. Morphological chart for a process capable of creating complex, hollow, metal geometries.

2.1. Substrate Removal

Substrate removal can be done through thermal means (e.g., burning out a thermoplastic), chemical means (e.g., etching away a photopolymer), or mechanical means (e.g., forcibly separating the substrate). Mechanical separation can only be done for very basic geometries and is not possible with the complex geometries investigated in this work, thus eliminating it from consideration. A thermal burnout process is ideal for materials that melt, which is why it is used in the investment casting process. It therefore works particularly well for waxes and thermoplastics (like ABS plastic and nylon, used in the FDM and SLS processes, respectively). This does not hold true for photopolymers (used in direct 3DP and stereolithography), which are thermosetting plastics that do not melt, instead violently expanding during burnout. While some research suggests that narrow channels in complex parts made from photopolymers can be removed after plating via chemical etching [19], the required etch changes with each photopolymer, of which there are many. The Objet photopolymers used in the direct 3DP process are not well-characterized, thus eliminating chemically etching as an option for 3DP parts. While etching is a possibility for SL parts, complexity is an issue. Etching chemicals must have access to the SL part. With a complex part that may include only one or two small entrances for etching chemicals, the etching process could take several days or weeks, assuming it is possible at all. Thermal substrate removal was therefore selected as the most reasonable substrate removal solution.

2.2. Additive Manufacturing

SL and direct 3DP parts are made of photopolymers. While the parts have very high resolution, they require extensive manual support removal after fabrication, which can be difficult or impossible to remove when producing complex structures. Additionally, testing showed that photopolymers violently expand as they are heated to the point of degradation. This expansion causes a great deal of internal pressure in the electroform, which catastrophically ruptured copper plating that was over $750\mu\text{m}$ thick, as shown in Figure 3. This chaotic thermal expansion eliminated both SL and 3DP from consideration in this procedure.

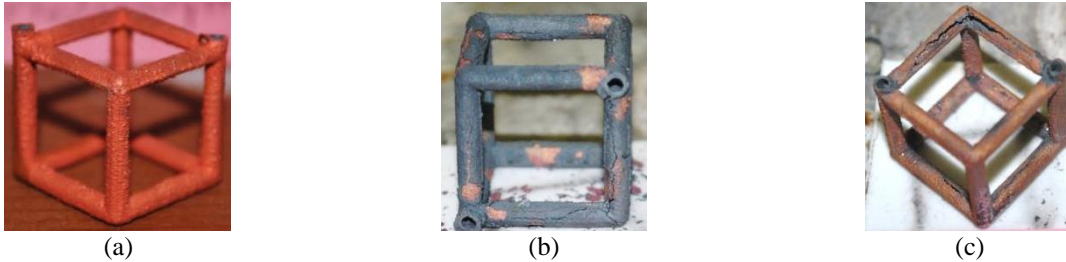


Figure 3. Burnout test of basic 3DP photopolymer part (with 20mm dimensions) after (a) copper electroplating, (b) burnout, (c) cleaning showing plate rupture.

FDM produces parts from thermoplastics, typically ABS. ABS is the most commonly electroplated and electrolessly plated type of polymer in industry because of the simplicity of etching before electroless nickel plating (ENP) [21]. As a thermoplastic, ABS provides the benefit of being able to melt during a potential burnout process. Unfortunately, the FDM process provides clear delineations between layers due to relatively large layer thicknesses (on the order of $254\mu\text{m}$), showing a “stair-stepping” effect on curves and angles. This effect precludes the use of the FDM process in the creation of complex geometries because angles and curves are a requirement for design freedom. As such, use of the FDM process was removed from consideration.

SLS most commonly produces parts from DuraForm™ PA (polyamide) powder, also known as Nylon 12. As a thermoplastic, polyamide is also a good candidate for a polymer burnout processes. Unfortunately, polyamide is rarely used for plating processes because it is hygroscopic, leading to potential warping when absorbing moisture during plating, so plating on nylon is not well-researched. As such, testing was performed to ensure that SLS parts could successfully be plated and burned out. Preliminary tests showed that SLS parts accept a conductive layer and a copper electroplate with a wax coating. The preliminary wax infiltration mitigated hygroscopy issues by pre-stressing the part, removing the possibility for detrimental structural changes during plating. The parts were successfully burned out from a $500\mu\text{m}$ thick copper electroplate without rupturing the plate. SLS was therefore selected as the most reasonable solution for the AM sub-function.

2.3. Metal Coating and Conductivizing

Vacuum Metallization, Metal Spraying, and Cathode Sputtering

Several technologies exist for coating metals onto polymer parts. Three widely used technologies are vacuum metallization, metal spraying, and cathode sputtering. In vacuum metallization, evaporated metal is condensed on the substrate. In metal spraying, metal is

atomized and propelled toward the substrate by a high velocity gas jet. In cathode sputtering, a high electrical potential disintegrate the surface of the source metal, projecting the disintegrated atoms onto the substrate. These three technologies each have high capital costs and can be very expensive for small batches of parts. Most importantly, they are each geometrically dependent, limiting their applicability for complex geometries. As such, they were eliminated from consideration in this process.

Electroplating and Conductivizing

Electroplating, also known as electrolytic plating, is a process in which an electrical current moves metal ions through an acid bath from a source metal (the anode) to the substrate (the cathode). Electroplating requires that the substrate have a conductive surface to complete the circuit. Conductivizing is typically done with either a base coat of electroless plating (usually nickel) or conductive silver paint. Preliminary tests showed that conductive paint provided a consistent conductive layer at a lower cost than ENP.

Electroplating is also a geometrically dependent process (the plate is thicker the closer the feature is to the anode), however the low cost and ease of use made it worthwhile to investigate. Extensive testing with copper electroplating showed that the electroplating process is considerably too geometrically dependent to be used in this process, as shown in Figure 4.

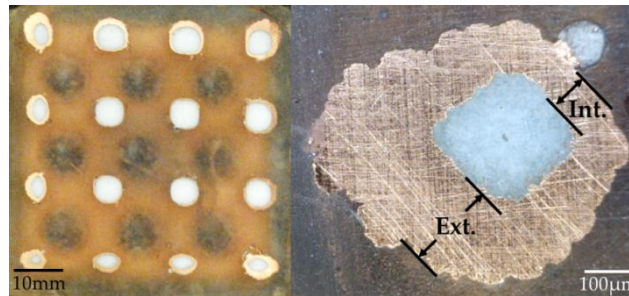


Figure 4. Cross-section of an electroplated part with a close up of the lower left strut showing the poor plate quality and large gradient from exterior (facing the anode) to interior (facing away from the anode).

The parts showed a considerable gradient from the exterior (closer to the anodes) to the interior. Even at high currents (which increase penetration into the part) with large entry pores, the copper did not plate all the way to the interior of the 48mm x 48mm x 48mm part, leaving an unplated region on the interior features of the central struts. Additionally, the plating quality was so low and unpredictable that the resultant parts would be useless for most applications. Due to these issues, electroplating was eliminated as a potential solution for the metal coating sub-function.

Electroless Plating

Electroless plating, also known as autocatalytic plating, is powered through a chemical reaction, as opposed to an electrical circuit. No anode is required as a source metal because the source metal is already present in the plating solution. This also means that the source metal in the solution must be periodically replenished as it is used. Deposition is provided by metal ions in the solution that are reduced to their metallic state in the presence of a reducing agent. ENP is most common and best understood. While electroless processes are more expensive than electroplating processes, they provide two advantages that are integral to this work. First, they

can plate on non-conductive surfaces with the proper pretreatment. Second, and most important, they do not depend on the geometry of the workpiece and provide an even plating coat regardless of the complexity of the part. Because of these advantages, electroless plating was selected as the solution for the metal coating sub-function.

3. PROCEDURE

From the review presented in Section 2, the selected morphological combination is shown in Figure 5. The proposed procedure begins with fabrication of a DuraForm™ polyamide part using SLS (Sinterstation 2500plus), followed by cleaning of excess powder with compressed air, then high pressure water cleaning. The part is then dried and degreased with acetone. The part is then etched with a sodium hydroxide (NaOH) solution [22], then undergoes a room temperature metallization (RTM) procedure for electrolessly plating a base coat of nickel onto the polymer (RTM kit for plastics from Transene, Inc.). After rinsing, the part is then submerged in a larger electroless nickel kit designed to plate nickel onto a base coat of nickel (ENP kit from Caswell, Inc.).

		Solutions				
Sub-Functions	Additive Manufacturing	Selective Laser Sintering (SLS)	Fused Deposition Modeling (FDM)	Direct Inkjet 3D Printing (3DP)	Stereolithography (SL)	
	Conductivizing	AgNO ₃ to Ag ₂ S Conversion	Conductive Paint (Silvaspray™)	Electroless Plating	None	
	Metal Coating	Electroplating	Vacuum Metallization	Metal Spraying	Cathode Sputtering	Electroless Plating
	Substrate Removal	Burnout (Thermal)		Etching (Chemical)	Separation (Mechanical)	

Figure 5. Updated morphological chart for process generation indicating which solutions are not feasible and indicating the selected morphological combination.

Because the plating nickel is present in the solution (as opposed to being in an anode), periodic chemical replenishment is necessary. Since the ability of electroless plating to produce thick coats is not well-researched, this experiment was also used to investigate if very thick coats were possible. As such, the part was allowed to plate until the bath was “killed”, having gradually degraded during the reaction. The resultant plate thickness was about 800µm, showing that thick coats are possible with ENP. Such a thick coat required chemical replenishments every 100 minutes.

The plated part underwent a flash burnout procedure for substrate removal. In this process, the part is heated well above the temperature at which most of the mass is degraded in a very short period, essentially shocking the material into degradation before it is allowed to expand significantly. A custom-built gas fired kiln in Virginia Tech’s Kroehling Advanced Materials Foundry was used for this procedure. The part was placed in the furnace, which ramped from room temperature up to 750°C (180°C greater than the temperature at which 96% of the polyamide should degrade [23]) in about five minutes. The part was left at this temperature for 15 minutes, then allowed to cool for about 20 minutes before opening the furnace. Additional procedural details are presented in [24].

4. RESULTS AND ANALYSIS

To evaluate the ENP process, tests were conducted on a 3mm pore diameter part. The full size (48mm cubed) part underwent the fabrication, cleaning, etching, and RTM base coat. The RTM ENP solution produced large bubbles (on the order of about 3mm in diameter) that had a tendency to become trapped in the interior of the part, requiring agitation to continue plating. This process deposited a nickel plate between 5 and 10 μ m thick. The part was then bisected, which confirmed that there was consistent plating throughout. The part was then further sectioned down to dimensions of 21mm x 22.5mm x 25.5mm.

The progress of the main plate over time was evaluated by analyzing images taken at specific times, providing a coarse estimate of the plating rate in the ENP bath. Examples of these images are shown in Figure 6.

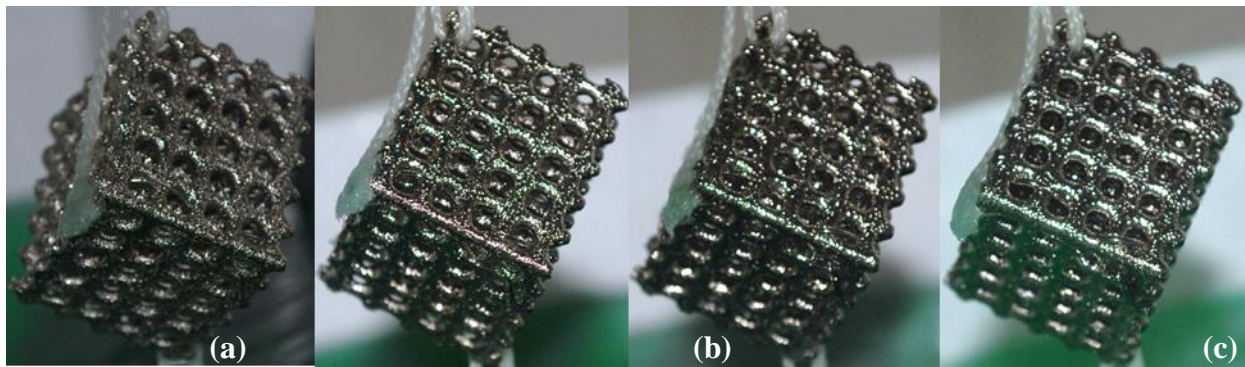


Figure 6. 3mm pore diameter part section during main ENP coating at (a) 0h50m, (b) 6h50m, (c) 11h50m, and (d) 15h10m.

After 24 hours of constant plating, the part had developed a plate thickness of about 800 μ m. The part plated at an average rate of 39 μ m per hour (via linear approximation; $R^2 = 0.9415$). While the rate of plating is relatively linear over short ranges, for thick coatings, the surface area changes significantly enough that the rate of plate growth may decrease slightly (explaining the discrepancy between the plate thickness after 24 hours and the plating rate during the first 15 hours of plating). This plating rate is dependent upon the plating duration, the surface area of the part, and the volume of the ENP bath. The chemical proportions of the bath are determined by the surface area of the part, so while the plating rate would normally be constant no matter the surface area of the part, a significant surface area change during plating will slow the reaction. The degradation of the bath over time can have a similar effect. Larger volume baths will allow the part to plate faster.

After plating, the part was bisected, with one half being used to display the cross-section to ensure that plating occurred evenly throughout the part, shown in Figure 7. The cross-section was ground with increasing fineness from 240 grit to 1500 grit and inspected under a stereo microscope with oblique illumination.

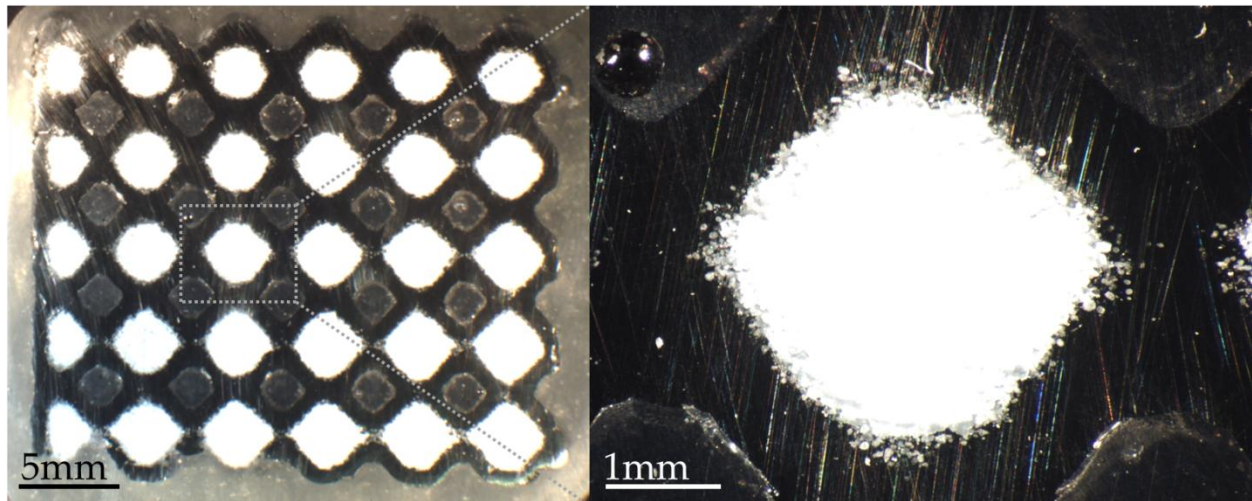


Figure 7. ENP cross-section and a micrograph of a single strut in the interior of the part prior to burnout.

There are some macro defects visible in the plate (e.g., missing plating on the bottom at the third strut) that are due to the bisection with a band saw before the epoxy was embedded, causing the nickel plate to break. The minimum and maximum plate thicknesses measured were $760\mu\text{m}$ and $820\mu\text{m}$. The part plated consistently throughout, providing no evidence of a trend in plate thickness dependent upon the part geometry.

When observed at a higher zoom with polarization under a different optical microscope, the plate shows a layering effect, visible in Figure 8.

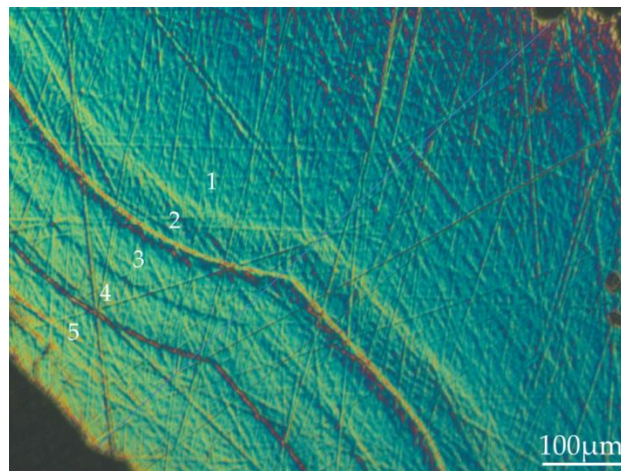


Figure 8. Polarized micrograph of a cross-section of the nickel plate showing plate layering with a SLS strut (black, top right) and an epoxy-filled pore (black, bottom left).

The straight-lined crisscrossed pattern is due to the grinding process. Five layers (labeled) are readily visible, though more may become visible with a finer polishing procedure. It is believed that these layers are caused by the ENP replenishment process. Extrapolating the width of the layers to include the range in which they are not visible in Figure 8 (moving from layer one to the nylon strut in the top right) provides a count of about 10 layers, the same as the number of replenishments during the plating process.

The uniformity between the layers shown indicates the consistency of the ENP process. The visible curvature is believed to be caused by an expected propagation of the surface roughness of the SLS part, leading to a part surface covered in small smooth nodules. This is better seen when closely viewing the surface of the part, shown in Figure 9.

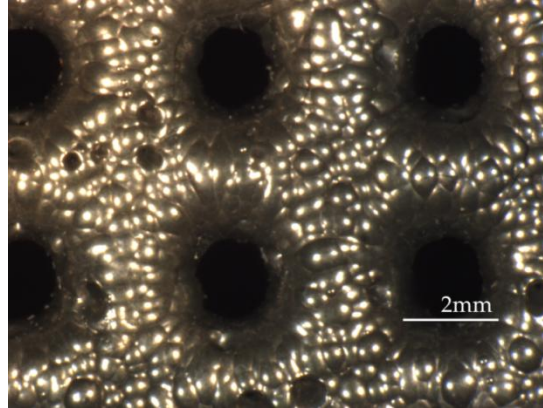


Figure 9. Micrograph of the surface finish of an ENP SLS part.

Also present are irregularly located holes in the plate, seen as black circles on the nickel surface on the left side of Figure 9. These holes do not penetrate through the entire plate and are believed to be caused by the collection of gas bubbles formed during the ENP reaction, keeping the solution from reaching specific locations on the plate. This problem could likely be solved with ultrasonic agitation of the bath, although agitation was not recommended by the plating bath manufacturer (Caswell, Inc.).

The second half of the bisected part moved to the burnout phase of the process with a flash burnout cycle in a gas fired kiln that heated from room temperature to 750°C in about 5 minutes, and then maintained temperature for 15 minutes. The furnace was then allowed to cool for about 20 minutes before being opened. The resultant complex, hollow, metal geometry is shown in Figure 10.



Figure 10. Successful complex, hollow, metal geometry made with SLS, ENP and flash burnout (27mm wide).

The breaks in the plate toward the top of the part are due to the bisecting process and were present before burnout began. With a nickel plate thickness of about 800 μm , the apparent density of this geometry is 3.16g/cm³ (less than half that of nickel at 8.9g/cm³), meaning that this structure is about 65 vol% air and 35 vol% nickel.

5. CLOSURE AND FUTURE WORK

The authors presented work scoping and designing a hybrid manufacturing procedure for producing complex, hollow, metal geometries with the design freedom of AM systems. Any geometry that can be produced with SLS can undergo this process, opening a new class of geometries to designers. Such geometries could be used for many applications, including novel heat exchangers and custom-fit high strength-to-weight ratio parts for structural supports or protective shielding.

The authors identified and summarized a new manufacturing procedure for creating complex, hollow, metal geometries. They produced a complex nickel cellular structure that is 65 vol% air with 3mm pores and 800 μm wall thicknesses. They used a polyamide substrate fabricated with selective laser sintering that underwent a three stage procedure of etching, room temperature metallization, and electroless nickel plating.

The developed process has some limitations qualitatively determined during experimentation. Parts with pores smaller than 3mm may encounter difficulty during the RTM ENP process due to the large bubbles created that can become trapped in the part. Since the part should not be agitated for the first few minutes of plating, the simple solution of agitation may not be possible. This also holds true for long channels that may hold air. The use of targeted low speed fluid pumps may help (perhaps running with an on/off duty cycle), but further investigation must be done to determine the associated detrimental effects to the start of plating.

Future work will investigate the use of copper electroless processes to take advantage of the benefits of higher heat conductivity for heat exchanger applications. In addition to exploring new material systems, the authors look next to the fabrication of well-researched geometries (e.g., an octet-truss structure) in order to better compare the mechanical properties of parts. Finally, the authors also look to the integration of part design with the process. Through collaborations with subject matter experts in fluid dynamics and heat transfer, the authors look to design a novel heat exchanger that can be compared to traditionally manufactured designs with standard metrics.

6. ACKNOWLEDGMENTS

The authors acknowledge Dr. Carlos Suchicital, of the Kroehling Advanced Materials Foundry of Virginia Tech, for his help with cross-sectioning parts and burnout procedures. The authors also acknowledge Kevin Kline for his work calibrating and operating the Sinterstation 2500plus. David McCarthy was supported by the Department of Defense as part of the SMART Scholarship Program.

7. REFERENCES

- [1] D. T. Queheillalt and H. N. G. Wadley, "Pyramidal lattice truss structures with hollow trusses," *Materials Science and Engineering: A*, vol. 397, pp. 132-137, 2005.
- [2] M. Rombouts, J. P. Kruth, L. Froyen, and P. Mercelis, "Fundamentals of Selective Laser Melting of alloyed steel powders," *CIRP Annals - Manufacturing Technology*, vol. 55, pp. 187-192, 2006.
- [3] S. Das, J. J. Beama, M. Wohlert, and D. L. Bourell, "Direct laser freeform fabrication of high performance metal components," *Rapid prototyping journal*, vol. 4, pp. 112-117, 1998.
- [4] E. Louvis, P. Fox, and C. J. Sutcliffe, "Selective laser melting of aluminium components," *Journal of Materials Processing Technology*, vol. 211, pp. 275-284, 2011.
- [5] I. Gibson, D. W. Rosen, and B. Stucker, *Additive Manufacturing Technologies*: Springer, 2010.
- [6] U. Chandrasekhar, K. Venkatesh, K. Elangovan, and T. Rangaswamy, "Integrated Use of Rapid Prototyping and Metal Plating Techniques for Development of Micro Air Vehicles," *International Journal of Engineering Science and Technology*, vol. 3, pp. 188-193, Jan 2011 2011.
- [7] N. Saleh, N. Hopkinson, R. J. M. Hague, and S. Wise, "Effects of electroplating on the mechanical properties of stereolithography and laser sintered parts," *Rapid prototyping journal*, vol. 10, pp. 305-15, 2004.
- [8] Z. Zhou, D. Li, Z. Zhengyu, and J. Zeng, "Design and fabrication of a hybrid surface-pressure airfoil model based on rapid prototyping," *Rapid prototyping journal*, vol. 14, pp. 57-66, 2008.
- [9] S. Markkula, S. Storck, D. Burns, and M. Zupan, "Compressive Behavior of Pyramidal, Tetrahedral, and Strut-Reinforced Tetrahedral ABS and Electroplated Cellular Solids," *Advanced Engineering Materials*, vol. 11, pp. 56-62, 2009.
- [10] M. D. Monzón, N. Diaz, A. N. Benitez, M. D. Marrero, and P. M. Hernandez, "Advantages of Fused Deposition Modeling for Making Electrically Conductive Plastic Patterns," in *2010 Sixth International Conference on Manufacturing Automation (ICMA 2010), 13-15 Dec. 2010*, Los Alamitos, CA, USA, 2010, pp. 37-43.
- [11] M. D. Monzón, M. D. Marrero, A. N. Benitez, P. M. Hernandez, and J. F. Cardenes, "A technical note on the characterization of electroformed nickel shells for their application to injection molds," *Journal of Materials Processing Technology*, vol. 176, pp. 273-277, 2006.
- [12] A. Arthur, P. M. Dickens, and R. C. Cobb, "Using rapid prototyping to produce electrical discharge machining electrodes," *Rapid prototyping journal*, vol. 2, pp. 4-12, 1996.
- [13] B. Yang and M. C. Leu, "Rapid electroforming tooling," *MRS proceedings*, vol. 625, pp. 57-66, 2000.
- [14] B. Yang and M. C. Leu, "Integration of Rapid Prototyping and Electroforming for Tooling Application," *CIRP Annals - Manufacturing Technology*, vol. 48, pp. 119-122, 1999.
- [15] F. Gillot, P. Mognol, and B. Furet, "Dimensional accuracy studies of copper shells used for electro-discharge machining electrodes made with rapid prototyping and the electroforming process," *Journal of Materials Processing Technology*, vol. 159, pp. 33-39, 2005.

- [16] D. E. Dimla, N. Hopkinson, and H. Rothe, "Investigation of complex rapid EDM electrodes for rapid tooling applications," *The International Journal of Advanced Manufacturing Technology*, vol. 23, pp. 249-255, 2004.
- [17] A. J. Jacobsen, W. Barvosa-Carter, and S. Nutt, "Micro-scale Truss Structures formed from Self-Propagating Photopolymer Waveguides," *Advanced Materials*, vol. 19, pp. 3892-3896, 2007.
- [18] A. J. Jacobsen, "Optically Oriented Three-Dimensional Polymer Microstructures," USA Patent, 2010.
- [19] T. A. Schaedler, A. J. Jacobsen, A. Torrents, A. E. Sorensen, J. Lian, J. R. Greer, L. Valdevit, and W. B. Carter, "Ultralight Metallic Microlattices," *Science*, vol. 334, pp. 962-965, November 18, 2011.
- [20] H. Wei, G. D. Hibbard, G. Palumbo, and U. Erb, "The effect of gauge volume on the tensile properties of nanocrystalline electrodeposits," *Scripta Materialia*, vol. 57, pp. 996-999, 2007.
- [21] R. Parkinson, "Plating on plastics. An industry review," *Plating and Surface Finishing*, vol. 81, pp. 32-35, 1994.
- [22] P. A. Schweitzer, *Fundamentals of Corrosion: Mechanisms, Causes, and Preventative Methods*, 1 ed.: CRC Press, 2009.
- [23] M. Vasquez, B. Haworth, and N. Hopkinson, "Optimum sintering region for laser sintered nylon-12," *Proceedings of the Institution of Mechanical Engineers. Part B, Journal of engineering manufacture*, vol. 225, pp. 2240-2248, 2011.
- [24] D. L. McCarthy, "Creating Complex Hollow Metal Geometries Using Additive Manufacturing and Metal Plating," Master of Science, Mechanical Engineering, Virginia Polytechnic Institute and State University, 2012.